Preprints of the 20th World Congress
The International Federation of Automatic Control
Toulouse, France, July 9-14, 2017

Reconfigurable Control Design of Steering and Torque Vectoring Based on Reachability Set Analysis ⋆

Balázs Németh * **Péter Gáspár** ** **Dániel Fényes** *
József Bokor **

* *Institute for Computer Science and Control, Hungarian Academy of Sciences, Kende u. 13-17, H-1111 Budapest,Hungary*
** *Institute for Computer Science and Control, Hungarian Academy of Sciences and MTA-BME Control Engineering Research Group*
E-mail: balazs.nemeth@sztaki.mta.hu

Abstract: The paper proposes a reconfigurable control design of steering and torque vectoring using a variable-geometry suspension system. Torque vectoring control is based on the independent driving of the wheels. Simultaneously, the steering angle is generated by the variable-geometry suspension system by varying the camber angle of the front wheels. The efficiency of wheel tilting and torque vectoring, and their coordinated actuation are in the focus of the paper. In the analysis a reachable set computation method on the polynomial model of the vehicle based on the trajectory reversing method and the Sum-of-Squares (SOS) programming is proposed. Based on the analysis results a reconfigurable control is designed using the Linear Parameter Varying (LPV) method.

Keywords: Variable-geometry suspension; Torque-vectoring; Reachability analysis; Reconfigurable control.

1. INTRODUCTION AND MOTIVATION

In the paper the maneuvers are executed by the variable-geometry suspension system. The advantages of the variable-geometry suspension are the simple structure, low energy consumption and low cost compared to other mechanical solutions such as an active front wheel steering, see Evers et al. [2008], Lee et al. [2005]. There are several application possibilities for the variable-geometry suspensions. The active tilt control system which assists the driver in balancing the vehicle and performs tilting in the bend is an essential part of a narrow vehicle system, see Piyabongkarn et al. [2004]. The novelty of the paper is the application of the variable-geometry suspension in both steering and trajectory tracking.

The in-wheel electric drive poses new challenges in generating the differential yaw moment of the vehicle. The independent steering control for the rear wheels to modify the toe angle was presented by Lee et al. [1999], Ronci et al. [2011]. The independent, fast and precise torque generation of the hub motors lends torque vectoring capability to the vehicle with which maneuverability can be enhanced significantly, see Wu et al. [2013], Shuai et al. [2013], Castro et al. [2012]. By knowing the characteristics of the in-wheel motors and the hydraulic brake system, energy optimal torque distribution and high efficiency regenerative braking can be implemented, as proposed by Cheng and Xu [2015], Wang et al. [2014] A fault-tolerant control system designed to accommodate hub motor faults by automatically reallocating the control effort among other healthy wheels was proposed by Wang and Wang [2012], Hu et al. [2011].

In the paper a new conception of integrated steering and driving is proposed, which is based on the coordination of steering and torque vectoring using the variable-geometry suspension system. The purpose of the variable-geometry suspension control is the modification of the geometry, which results in a change in the camber angle and the position of the wheel-road contact. Thus, the scrub radius is also modified. Consequently, a longitudinal force on the wheel creates a moment on the wheel and, thus, realizes the steering angle.

Another contribution of the work is the reachability analysis of the control interventions. The method results in a theoretical basis for the necessity of the reconfiguration and the efficiency of the coordination. Moreover, a reconfigurable Linear Parameter-Varying (LPV) control of the system is presented, which is able to coordinate wheel tilting, steering and the longitudinal driving/braking forces on the wheels through a reconfiguration strategy. In an earlier paper the integration possibility of the variable-geometry suspension and driving was also examined in Németh et al. [2016a].

The structure of the paper is the following. The modeling of the lateral dynamics incorporating the steering dynam-

⋆ The research was supported by the National Research, Development and Innovation Fund through the project "SEPPAC: Safety and Economic Platform for Partially Automated Commercial vehicles" (VKSZ 14-1-2015-0125). This paper was partially supported by the János Bolyai Research Scholarship of the Hungarian Academy of Sciences.

ics is presented in Section 2. The reachability analysis of the suspension-based steering and the torque vectoring are proposed in Section 3. The control design of the controllers and their reconfiguration strategy are presented in Section 4. The operation of the reconfiguration strategy is illustrated through the CarSim simulation environment in Section 5.

2. MODELING OF THE LATERAL VEHICLE DYNAMICS

The scheme of the variable-geometry suspension is shown in Figure 1. The actuator is incorporated in the suspension between the wheel hub and the wheel. It is able to generate an active torque M_{act} to tilt the wheel. However, it also has a counter effect $-M_{act}$ on the hub. In the suspension construction is able to rotate around the connection point of the chassis. Moreover, the arm connects the hub and the chassis with joints, which are able to guarantee the rotation and the motion of the suspension.

The goal of the modeling of the lateral vehicle dynamics is to formulate the relationships between the wheel camber angle γ, the longitudinal wheel force $F_{l,i}$ and the vehicle motion. Since $F_{l,i}$, $i \in \{l, r\}$ has an effect on maneuvering through torque vectoring and γ through the steering angle, both of the interventions in the dynamical equations are incorporated.

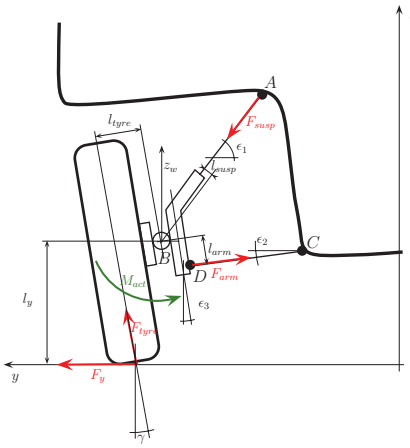

Fig. 1. Scheme of the suspension construction

The lateral motion of the vehicle is described by the following equations, see Rajamani [2005]:

$$J\ddot{\psi} = \mathcal{F}_1(\alpha_1)l_1 - \mathcal{F}_2(\alpha_2)l_2 + M_d, \tag{1a}$$

$$mv\left(\dot{\psi} + \dot{\beta}\right) = \mathcal{F}_1(\alpha_1) + \mathcal{F}_2(\alpha_2), \tag{1b}$$

where m is the vehicle mass, J is the yaw-inertia of the vehicle, l_1 and l_2 are geometric parameters, C_1 and C_2 are cornering stiffness values, $\dot{\psi}$ is the yaw rate of the vehicle, β is the side-slip angle and M_d is the differential yaw moment. $\mathcal{F}_i$ represents the lateral forces on the front and rear wheels. The side-slip angles of the front and rear axles α_1 and α_2 are expressed: $\alpha_1 = \delta - \beta - \dot{\psi}l_1/v$ and $\alpha_2 = -\beta + \dot{\psi}l_2/v$. In the single-track model δ represents the steering wheel, generated through γ. The vehicle model (1) can be reformulated as follows:

$$\dot{\alpha}_2 - \dot{\alpha}_1 = \left[\frac{l_1 + l_2}{Jv}\left(\mathcal{F}_1(\alpha_1)l_1 - \mathcal{F}_2(\alpha_2)l_2\right)\right] - \\ - \dot{\delta} + \frac{l_1 + l_2}{Jv}M_d, \tag{2a}$$

$$\dot{\alpha}_1 l_2 + \dot{\alpha}_2 l_1 = v(\alpha_2 - \alpha_1) - \frac{l_1 + l_2}{mv}\left[\mathcal{F}_1(\alpha_1) + \mathcal{F}_2(\alpha_2)\right] + \\ + v\delta + l_2\dot{\delta}. \tag{2b}$$

In the reformulated equations the side-slips α_1, α_2 are the states of the system. Thus, the vehicle model is transformed to a state-space representation as below:

$$\dot{x} = \begin{bmatrix}\dot{\alpha}_1 \\ \dot{\alpha}_2\end{bmatrix} = \begin{bmatrix}\mathrm{f}_1(\alpha_1, \alpha_2) \\ \mathrm{f}_2(\alpha_1, \alpha_2)\end{bmatrix} + \begin{bmatrix}g_1 \\ g_2\end{bmatrix} M_d + \begin{bmatrix}h_{11}h_{12} \\ h_{21}h_{22}\end{bmatrix} \begin{bmatrix}\dot{\delta} \\ \delta\end{bmatrix} = \\ = f(x) + gM_d + h\Delta. \tag{3}$$

In the modeling of the vehicle, the lateral forces are formulated as polynomials, such as $\mathcal{F}(\alpha) = \sum_{k=1}^{n} c_k\alpha^k = c_1\alpha + c_2\alpha^2 + \ldots + c_n\alpha^n$, where c_i coefficients are constants, see Németh et al. [2016b].

The description of the vehicle motion also requires the relations of the actuation interventions M_d and γ_i. First, the relation between the longitudinal force on the wheels and M_d is presented. $F_{l,i}$ influence not only the lateral motion of the vehicle, but also the longitudinal dynamics, e.g. the velocity profile. Moreover, the cruise control of vehicle also generates longitudinal force requirement F_0, which is an external signal for the lateral control system. the longitudinal forces on either side can be calculated from the following expressions: $F_{l,l} = F_0 + M_d/b_f$ and $F_{l,r} = F_0 - M_d/b_r$.

Second, the interconnection between γ and δ is formulated. The steering rotation of a wheel is described by the following dynamical equation: $\ddot{\delta}_i = r_{\delta,i}F_{l,i}/J_{\delta,i}$, $i \in \{l, r\}$, where $r_{\delta,i}$ is the scrub radius, $F_{l,i}$ is the longitudinal traction/braking force on the wheel, $J_{\delta,i}$ is the inertia of the steering system for one wheel. Moreover, there is a relationship between the steering angle and the longitudinal force. In practice, the relationship between $r_{\delta,i}$ and γ_i can be formulated linearly: $r_{\delta,i} = \varepsilon\gamma_i$, where ε is a construction parameter. The steering rotations of the wheels are extended to the lateral motion of the vehicle:

$$\ddot{\delta}_i = \frac{\varepsilon F_{l,i}}{J_{\delta,i}}\gamma_i, \quad i \in \{l, r\}. \tag{4}$$

These relations show the interconnections between the control interventions of the systems, such as the steering angle, the differential yaw moment and the longitudinal force.

3. REACHABLE SET ANALYSIS OF THE SYSTEM

The interventions of wheel tilting and torque vectoring result in the lateral motion of the vehicle. Since both actuations have an impact on the lateral dynamics, it is necessary to examine what the difference between their effects is. In this section an analysis on the set of states is presented, which can be reached through limited control input.

Formally, the set of the reachable states is defined in Boyd et al. [1997]. Given is a continuous-time system $\dot{x} = f(x(t)) + gu(t)$ with the initial condition $x(0) = 0$.

It is considered the set of reachable states with bounded inputs:

$$\mathcal{R} \triangleq \left\{ x(T) \;\middle|\; \begin{array}{l} (x(t), M_d(t), \Delta(t)) \,| \\ \\ \dot{x}(t) = f(x(t)) + gM_d(t) + h\Delta(t), x(0) = 0, \\ \Delta_{min} \leq \Delta(t) \leq \Delta_{max}, \\ M_{d,min} \leq M_d(t) \leq M_{d,max}, T \geq 0 \end{array} \right\} \quad (5)$$

The intervention of the variable-geometry suspension depends on two kinds if dynamics, such as the generation of the steering angle (4) and the effect of steering/torque vectoring on the vehicle motion (7). Although these dynamics can be combined through Δ, it results in a system with an increased number of states. Since the increase in the system complexity can be disadvantageous for numerical reasons, the reachable sets are computed separately in the following way.

The reachability of the steering dynamics can be computed analytically. The $\delta_i, \dot{\delta}_i$ solutions of the steered wheel, which is described by (4), are formed as

$$\dot{\delta}_i(t) = \frac{\varepsilon F_{l,i}}{J_{\delta,i}} t\gamma_i(t) \quad (6a)$$

$$\delta_i(t) = \frac{\varepsilon F_{l,i}}{2J_{\delta,i}} t^2\gamma_i(t) \quad (6b)$$

where $F_{l,i}$ is fixed. Moreover, the time domain is bounded to $t = T$, in which the reachability of the system $\dot{\delta}_i(T), \delta_i(T)$ is analyzed. Thus, (7) is reformulated as

$$\dot{x} = f(x) + gM_d + H(F_{l,i}, T)\gamma \quad (7)$$

In the following the computation of the reachable set is based on the trajectory reversing method Horiuchi [2015]. It means that the null-controllability region of the forward-time nonlinear system is equivalent to the reachability region of the reverse-time system Snow [1967]. The reverse-time system is formed as

$$\dot{x} = -f(x) - gM_d - H(F_{l,i}, T)\gamma \quad (8)$$

The advantage of the method is the computation of the controllability set for polynomial systems. Németh et al. [2016b] proposes a Sum-of-Squares programming based method, by which the controllability set of the polynomial system (8) can be computed. In the following the reachable set computation method based on the trajectory reversing method is discussed briefly.

The set computation method requires the existence of a smooth, proper and positive-definite Control Lyapunov Function $V : \mathbb{R}^n \to \mathbb{R}$, which requires that $\inf_{u\in\mathbb{R}} \left\{ \frac{\partial V}{\partial x}(-f(x)) + \frac{\partial V}{\partial x}(-M) \cdot u \right\} < 0$ must be guaranteed for each $x \neq 0$, where $M = [g\ H]$ and $u = [M_d\ \gamma]^T$. The inequality can be guaranteed at different scenarios, considering $u = \{-u_{max}; u_{max}\}$.

1/ If $\frac{\partial V}{\partial x}(-f(x)) < 0$ then the system is stable and $u \equiv 0$. This stability scenario is contained by the next two stability criteria.
2/ If $\frac{\partial V}{\partial x}(-f(x)) > 0$ then the system is unstable. However, the system can be stabilized If $\frac{\partial V}{\partial x} g < 0$ and $\frac{\partial V}{\partial x}(-f(x)) + \frac{\partial V}{\partial x}(-g) \cdot u_{max} < 0$, then the lower peak-bound of control input u stabilizes the system. If $\frac{\partial V}{\partial x} g > 0$ and $\frac{\partial V}{\partial x}(-f(x)) - \frac{\partial V}{\partial x}(-g) \cdot u_{max} < 0$, then the upper peak-bound of control input u stabilizes the system.

The stability criterion of the polynomial system leads to set emptiness conditions, which can be transformed into an SOS optimization problem using the generalized S-Procedure Thus, the next optimization problem is formed to find the maximum Controlled Invariant Set:

$$\max \beta \quad (9)$$

over SOS polynomials $s_1, s_2, s_3, s_4, s_5 \in \Sigma_n$ and polynomials $V, p_1, p_2 \in \mathcal{R}_n,\ V(0) = 0$ such that

$$-\left(-\frac{\partial V}{\partial x} f(x) + \frac{\partial V}{\partial x} g\ u_{max}\right) - s_1\left(-\frac{\partial V}{\partial x} g\ - \epsilon\right) - \\ - s_2(1 - V) - p_1 L_1 \in \Sigma_n \quad (10a)$$

$$-\left(-\frac{\partial V}{\partial x} f(x) - \frac{\partial V}{\partial x} g\ u_{max}\right) - s_3\left(\frac{\partial V}{\partial x} g\ - \epsilon\right) - \\ - s_4(1 - V) - p_2 L_2 \in \Sigma_n \quad (10b)$$

$$- s_5(\beta - p) - (V - 1) \in \Sigma_n \quad (10c)$$

where $L_{1,2}(x)$ is chosen as a positive definite polynomial, $\epsilon \in \mathbb{R}^+$ is as small as possible, $p \in \Sigma_n$ is a fixed and positive definite function and β defines a $P_\beta := \{x \in \mathbb{R}^n | p(x) \leq \beta\}$ level set.

Illustration of the reachable sets

The efficiency of the reachable set computation method in Figure 2 is illustrated. The example on the set of the wheel tilting is computed at $F_l = 750N$ and $T = 0.1s$. In the approximation of the reachability domain a 6^{th}-order polynomial Control Lyapunov Function is used. In the example a simulation is used in which the system is actuated through a chirp signal with the maximum amplitude $\gamma = 1.5°$. The adhesion coefficients between the wheels and the road are considered as $\mu = 0.9$, while the vehicle speed is $v = 20m/s$. The presented results show that the reachable set approximates the reachability domain appropriately.

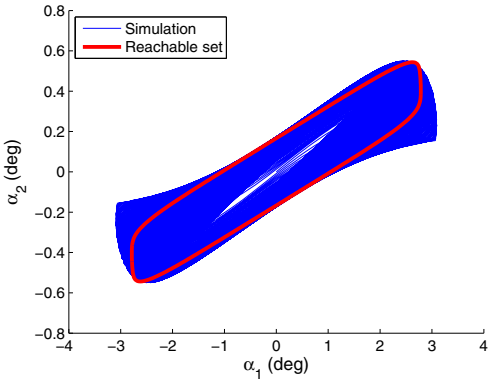

Fig. 2. Example on reachable set computation

The reachable sets of the system are computed for the actuations γ_i and M_d. In Figure 3 the reachable sets for different F_l longitudinal forces are illustrated. The maximum actuation is $\gamma = \pm 1.5°$. It can be seen that the intervention possibility of the system is influenced significantly by F_l. The results demonstrate that in the case of $F_l = 0$ scenario the reachable set is zero, thus the actuation of the camber angle is ineffective. However, if F_l is increased, the reachability of the system also improves. The reachable sets of the torque vectoring intervention for different

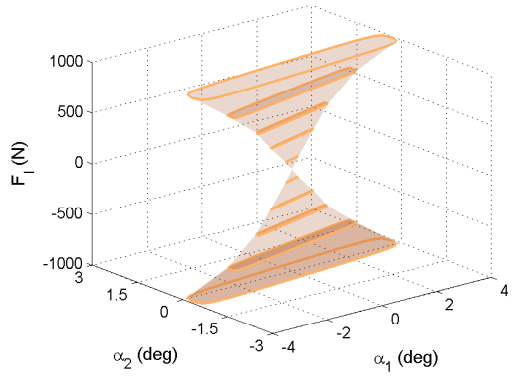

Fig. 3. Reachable sets of the variable-geometry suspension

maximum M_d torque values are shown in Figure 4. The results show that the shape of the sets is different from the reachability domain of the variable-geometry suspension. The differences in the sets lead to the possibility of the reconfiguration between the wheel tilting actuation and the torque vectoring. Finally, the reachability analysis is

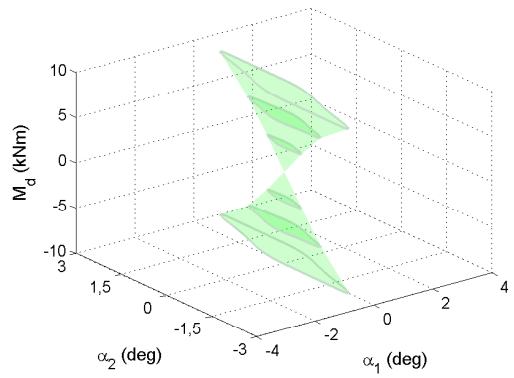

Fig. 4. Reachable sets of the torque vectoring

examined on the integrated actuation of wheel tilting and torque vectoring, see Figure 5. In this case the maximum camber angle $\gamma = \pm 1.5°$ and $M_d = 9000Nm$ are applied on the vehicle. The results show that the reachable sets of the system with the integrated actuation can be significantly increased. In the case of the integrated intervention the efficiency of the vehicle control system at all F_l values can be guaranteed.

The presented analysis results show that the suspension-based steering and the torque vectoring have different impacts on the reachability of the vehicle control. Through wheel tilting α_1 can be increased, while the torque vectoring has significant effect on α_2. Moreover, the impact of γ depends significantly on the longitudinal force on the wheels. However, the coordinated interventions of the actuators can guarantee the significant increase in the reachability domain.

4. RECONFIGURABLE CONTROL DESIGN OF THE SYSTEM

In this section the reconfigurable control design of the suspension-based steering and the torque vectoring is

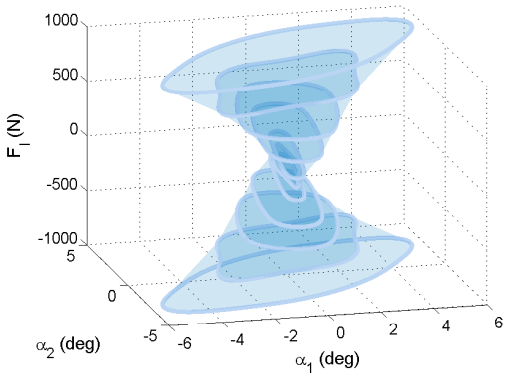

Fig. 5. Reachable sets of the integrated actuation

proposed. Since the reachable set analysis shows that the system is able to operate in a limited α_1, α_2 region, the linear approximation of the system models results in acceptable control-oriented vehicle models.

Control of steering wheel dynamics

The state-space representation of the steering wheel dynamics from (4) is formed as

$$\dot{x}_{st,i} = A_{st}x_{st,i} + B_{st,i}(F_{l,i})u_{st,i} \tag{11}$$

where $A_{st}, B_{st,i}(F_{l,i})$ are matrices, $x_{st,i} = \left[\dot{\delta}_i \ \delta_i\right]^T$ and $u_{st,i} = \gamma_i$.

The purpose of the steering control is to guarantee the tracking of the reference steering signal $\delta_{ref} = \delta$, which is computed through the lateral controller:

$$z_{st,i,1} = \delta_{ref} - \delta_i, \quad |z_{st,i,1}| \to min \tag{12}$$

Moreover, the performance $z_{st,1}$ must be reached using minimum control input:

$$z_{st,i,2} = \gamma_i, \qquad |z_{st,i,2}| \to min \tag{13}$$

The performances are formed in a vector, such as $z_{st,i} = [z_{st,i,1};\ z_{st,i,2}]^T$. Moreover, $y_{st} = \delta_i$ is the measured signal.

The purpose is to design controllers for both the left and the right wheels based on LPV method. The design is based on a weighting strategy, which is formulated through a closed-loop interconnection structure. The purpose of weighting functions $W_{st,1}$ and $W_{st,2}$ are to define the performance specifications in such a way that a trade-off is guaranteed between $z_{st,i,1}$ and $z_{st,i,2}$. The weight of $z_{st,i,1}$ is chosen in the form $W_{st,1} = A_{st,1}/(T_{st,1}s + 1)$, which scales the admissible tracking error. The actuation γ_i is scaled with the function in the form $W_{st,2} = A_{st,2}$, which determines the amplitude of the control signal. The aim of the function $W_{st,ref} = A_{st,3}$ is to scale the reference signal δ_{ref}. The control design is based on the LPV method that uses parameter-dependent Lyapunov functions, see Bokor and Balas [2005], Wu et al. [1996].

Control of lateral dynamics

The goal of the integrated control design is to guarantee trajectory tracking and the robust stability of the entire system through the computation of the control inputs δ_{ref}

and M_d. The lateral dynamics of the vehicle from (1) is formed as

$$\dot{x}_{lat} = A_{lat}x_{lat} + B_{lat}u_{lat} \tag{14}$$

where A_{lat}, B_{lat} are matrices, $x_{lat} = \begin{bmatrix}\dot{\psi} & \beta\end{bmatrix}^T$ and $u_{lat} = \begin{bmatrix}\delta & M_d\end{bmatrix}^T$ and $\delta = (\delta_l + \delta_r)/2$. The vehicle must follow a reference yaw-rate signal $\dot{\psi}_{ref}$. The performance is defined as

$$z_{lat,1} = \dot{\psi}_{ref} - \dot{\psi}, \quad |z_{lat,1}| \to min \tag{15}$$

where $\dot{\psi}_{ref}$ is computed using the velocity and the steering wheel angle of the driver, see Rajamani [2005]. Moreover, the performance $z_{lat,1}$ must be reached using minimum control input $u_{lat} = [\delta_l;\ \delta_r;\ M_d]^T$. Thus, the further two performances are defined:

$$z_{lat,2} = \begin{bmatrix}\delta_l & \delta_r\end{bmatrix}^T, \quad |z_{lat,2}| \to min \tag{16a}$$

$$z_{lat,3} = \begin{bmatrix}M_d\end{bmatrix}^T, \quad |z_{lat,3}| \to min \tag{16b}$$

The performances are compressed in a vector $z_{lat} = [z_{lat,1};\ z_{lat,2};\ z_{lat,3}]^T$. Moreover, the measured signal is $y_{lat} = \dot{\psi}$.

In the architecture three performance weighting functions are used. While $W_{lat,1}$ scales the admissible error on the yaw-rate tracking, the weights $W_{lat,2}(\rho_{lat})$ and $W_{lat,3}$ have impact on the actuation. The weight on the steering angle is selected as parameter-dependent, in the following form: $W_{lat,2}(\rho_{lat}) = \rho_{lat}/A_{lat,2}$, where $\rho_{lat} \in [\rho_{lat,min}, \rho_{lat,max}]$ is a scheduling variable of the system. The role of ρ_{lat} is to influence the actuation of the variable-geometry suspension through the steering intervention. In the case of small $|F_{l,i}|$ values the camber angle has a low impact on the steering angle and the vehicle dynamics. Therefore, the vehicle motion must be influenced through the differential yaw moment instead of δ_{ref}. The reconfiguration is guaranteed by the selection of ρ_{lat}. If $\rho_{lat} = \rho_{lat,min}$, then $W_{lat,2}(\rho_{lat,min})$ has a small value, which results in the increase of δ_{ref}. Similarly, if $\rho_{lat} = \rho_{lat,max}$, then $W_{lat,2}(\rho_{lat,max})$ has a high value, which reduces the steering actuation. The weight on M_d is selected a constant value, such as $W_{lat,3} = A_{lat,3}$. Thus, the trade-off between the actuation of δ_{ref} and M_d is determined by ρ_{lat}.

Reconfiguration strategy and architecture of the systems

The reconfiguration strategy in the control of variable-geometry suspension and torque vectoring is based on the selection of ρ_{lat}. In Section 3 the analysis shows that the torque vectoring and the suspension-based steering have different reachable sets. Moreover, F_l significantly influences the reachable sets of the variable-geometry suspension. However, the integration of the actuations improves the maneuvering capabilities of the vehicle. The consequences of the analysis motivate the construction of a reconfiguration strategy, which is presented below.

The role of the reconfiguration strategy is to avoid the significant reduction in the reachable sets. Based on the wheel tilting analysis, the small longitudinal forces on the wheels lead to decreased sets, see Figure 3. Therefore, the decision on the reconfiguration is based on the value of F_l. The reconfiguration between γ and M_d is realized through the scheduling variable ρ_{lat}, which is built in the control of lateral dynamics.

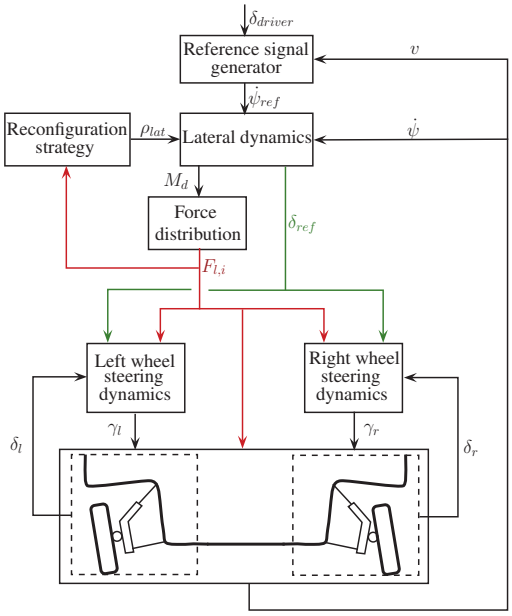

Fig. 6. Architecture of the system hierarchy

Since the low values of $|F_{l,i}|$ have a disadvantageous effect on the vehicle dynamics, $\rho_{lat,max}$ is selected if $|F_{l,i}| < F_{min}$, where F_{min} and F_{max} are design parameters. If $|F_{l,i}| > F_{max}$ then the actuation of the steering is preferred. The role of the section between F_{min} and F_{max} is to avoid the chattering in the steering signal.

The hierarchy of the reconfigurable control is illustrated in Figure 6. It presents that the reconfiguration strategy has an impact on the lateral dynamics, which results in the generation of M_d and δ_{ref}. The computed torque is distributed to longitudinal control forces, while δ_{ref} is the reference signal of the wheel steering control. The reference trajectory of the entire vehicle control system is designed through the velocity of the vehicle and the cornering intention of the driver, estimated from the steering wheel angle δ_{driver}.

5. SIMULATION EXAMPLE

The efficiency of the variable-geometry suspension control system is presented through a simulation example. Its purpose is to show the operation of the hierarchical control system, which is able to guarantee the tracking performances. In the simulation a mid-size passenger car with varying velocity is driven along an S-curve of the Albert Park Circuit, located near Melbourne, Australia.

The longitudinal wheel forces, which vary during the simulation, are shown in Figure 7(a). The yaw-rate tracking of the control system is presented in Figure 7(b). It is shown that the accuracy of the control system is independent of the variation of $F_{l,i}$. The interventions of both the steering angle and differential yaw moment are shown in Figure 7(c),(d). The scheduling variable ρ_{lat} guarantees the reconfiguration strategy of the interventions, see Figure 7(e). Moreover, ρ_{lat} is in relation with $F_{l,i}$, see e.g. the section $0 \ldots 100m$, where the varying longitudinal force influences the scheduling variable significantly. It results in the modification of the coordination of the control signals, δ_{ref} and M_d. The realization of the left/right wheel

steering angles is based on the tilting of the wheel, see Figure 7(f). It demonstrates that the steering based on the variable-geometry system requires a small camber angle, which is an advantage of the designed system. Finally, it

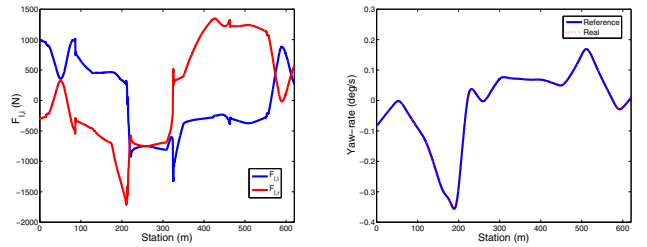

(a) Longitudinal wheel forces (b) Yaw-rate tracking

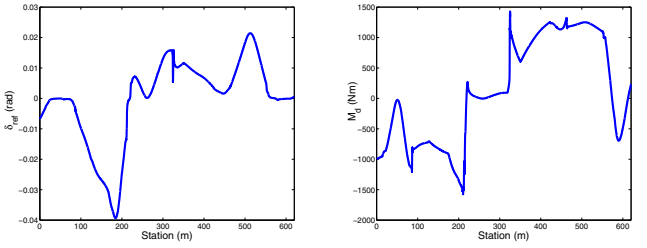

(c) Steering angle (d) Differential yaw moment

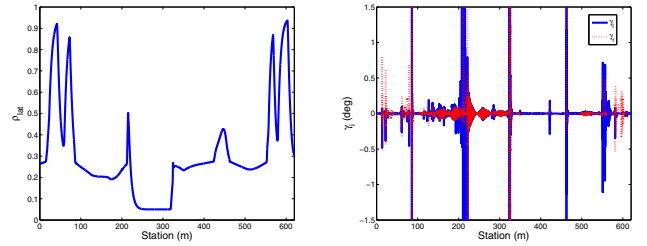

(e) Scheduling variable (f) Camber angle

Fig. 7. Signals of the trajectory tracking

can be concluded that the proposed hierarchical control structure is able to guarantee the tracking performances of the system. In the reconfiguration strategy steering and torque vectoring are operated in cooperation, which results in an adequate maneuvering capability of the vehicle.

6. CONCLUSIONS

In the paper a reconfigurable control design for steering and torque vectoring based on the variable-geometry suspension has been proposed. Torque vectoring control is based on the independent steering/driving wheel systems, while the steering angle is generated by the variable-geometry suspension system by modifying the camber angle at each wheel at the front. A reachable set computation method for the polynomial system of the vehicle based on the trajectory reversing method has been proposed. It has been demonstrated that wheel tilting and torque vectoring have different impacts on the reachability domain of the vehicle. Moreover, the set of the suspension depends significantly on the longitudinal forces on the wheels. However, the coordinated intervention leads to an increase in the reachable sets.

REFERENCES

J. Bokor and G. Balas. Linear parameter varying systems: A geometric theory and applications. *16th IFAC World Congress, Prague*, 2005.

S. Boyd, L. El Ghaoui, E. Feron, and V. Balakrishnan. *Linear Matrix Inequalities in System and Control Theory*. Society for Industrial and Applied Mathematics, Philadelphia, 1997.

R. Castro, R. E. Araújo, M. Tanelli, S. M. Savaresi, and D. Freitas. Torque blending and wheel slip control in evs with in-wheel motors. *Vehicle System Dynamics*, 50:71–94, 2012.

C. Lin Cheng and Z. Xu. Wheel torque distribution of four-wheel-drive electric vehicles based on multi-objective optimization. *Energies 2015*, 8:3815–3831, 2015.

W.J. Evers, A. van der Knaap, I. Besselink, and H. Nijmeijer. Analysis of a variable geometry active suspension. *International Symposium on Advanced Vehicle Control, Kobe, Japan*, 2008.

S. Horiuchi. Evaluation of chassis control algorithms using controllability region analysis. *International Symposium on Dynamics of Road Vehicles on Roads and Tracks, Graz, Austria*, 2015.

J.-S. Hu, D. Yin, and Y. Hori. Fault-tolerant traction control of electric vehicles. *Control Engineering Practice*, pages 204–213, 2011.

H.S. Lee, U.K. Lee, S.K. Ha, and C.S. Han. Four-wheel independent steering (4wis) system for vehicle handling improvement by active rear toe control. *JSME International Journal Series C*, 42(4): 947–956, 1999.

S. Lee, H. Sung, and U. Lee. A study to the enhancement of vehicle stability by active geometry control suspension (agcs) system. *13th Int. Pacific Conference on Automotive Engineering, Gyeongju*, pages 1–6, 2005.

B. Németh, D. Fényes, P. Gáspár, and J. Bokor. Trajectory tracking based on independently controlled variable-geometry suspension for in-wheel electric vehicles. 55^{th} *IEEE Conference on Decision and Control, Las Vegas, USA, in print*, 2016a.

B. Németh, P. Gáspár, and T. Péni. Nonlinear analysis of vehicle control actuations based on controlled invariant sets. *Int. J. Applied Mathematics and Computer Science*, 26(1), 2016b.

D. Piyabongkarn, T. Keviczky, and R. Rajamani. Active direct tilt control for stability enhancement of a narrow commuter vehicle. *Int. J. Automotive Technology*, 5(2):77–88, 2004.

R. Rajamani. Vehicle dynamics and control. *Springer*, 2005.

M. Ronci, P. Artuso, and E. Bocci. Four independent wheels steering system analysis. *SAE Paper*, 2011. doi: 10.4271/2011-01-0241.

Z. Shuai, H. Zhang, J. Wang, J. Li, and M. Ouyang. Lateral motion control for four-wheel-independent-drive electric vehicles using optimal torque allocation and dynamic message priority scheduling. *Control Engineering Practice*, 24:55–66, 2013.

D. R. Snow. *Determining reachable regions and optimal controls*, volume 5 of *Advances in Control Systems*. Academic Press, 1967.

B. Wang, X. Huang, J. Wang, X. Guo, and X. Zhu. A robust wheel slip ratio control design combining hydraulic and regenerative braking systems for in-wheel-motors-driven electric vehicles. *Journal of the Franklin Institute*, 50:71–94, 2014.

R. Wang and J. Wang. Fault-tolerant control for electric ground vehicles with independently-actuated in-wheel motors. *Journal of Dynamic Systems, Measurement, and Control*, 134, 2012.

F. Wu, X. H. Yang, A. Packard, and G. Becker. Induced l^2-norm control for LPV systems with bounded parameter variation rates. *Int. J. Nonlinear and Robust Control*, 6:983–998, 1996.

F.-K. Wu, T.-J. Yeh, and C.-F. Huang. Motor control and torque coordination of an electric vehicle actuated by two in-wheel motors. *Mechatronics*, pages 46–60, 2013.